Supplementary Information (SI) for ChemComm.

# Supporting Information

# Diphosphine-induced morphological modification in Au nanoclusters and its implications for catalytic activity regulation

Jialing Li, Zhewei Wang, Jiansheng Ye, Qinzhen Li,* Sha Yang, Jinsong Chai and Manzhou Zhu*

Department of Chemistry and Centre for Atomic Engineering of Advanced Materials, Key Laboratory of Structure and Functional Regulation of Hybrid Materials of Ministry of Education, Institutes of Physical Science and Information Technology and Anhui Province Key, Laboratory of Chemistry for Inorganic/Organic Hybrid Functionalized Materials, Anhui University, Hefei, 230601, China
*E-mails of corresponding authors: qinzhenlee@163.com; zmz@ahu.edu.cn

## 1. Chemicals

All drugs required for this experiment are commercially available and used according to the received samples without further purification. Dichloromethane (DCM, HPLC grade), methanol (MeOH, HPLC grade), ethanol (EtOH, HPLC grade), toluene (TOL, HPLC grade), *n*-hexane (HPLC grade), 4-*tert*-butylphenylthiophenol (TBBT, ≥99%), 1,2-bis(diphenylphosphine)benzene (dppbe, ≥98%) $HAuCl_4.4H_2O$ (≥99.99%, metal based), borane *tert*-butylamine complex ($C_4H_{14}BN$, ≥95%) were all purchased from Shanghai McLean Biochemical Technology Co., Ltd. The round bottom flasks required in the experiment were rinsed with aqua regia and purified water before use.

## 2. Synthesis of $Au_{44}(TBBT)_{28}$

$Au_{44}(TBBT)_{28}$ was synthesized according to a previous report with some modifications.[1] Briefly, 400 µL of $HAuCl_4$ (0.2 g/mL in water) and 100 mg of TOAB were mixed in 5 mL of methanol, and the solution changes from yellow to red. After 5 min, 150 µL of TBBT dissolved in 10 mL of DCM was added, and the color of the solution changes from red to light yellow. After 20 min, 120 mg of borane *tert*-butylamine complex was added directly. The reaction gradually changes from light yellow to yellow brown, and finally to black. After stirring continuously at room temperature for 8 hours, the solvent was removed by rotary evaporation. The residue was washed with methanol, centrifuged, and the precipitate was collected. Then, the precipitate was redissolved with dichloromethane and centrifuged, the supernatant was retained and dried by rotary evaporation. This raw product was then dissolved in 2 mL of toluene with the addition of 100 µL TBBT. The reaction was then kept at 60 °C for 8 hours to proceed the etching process. After that, the solvent was evaporated and the residue was washed twice with methanol. Then, the raw product was further purified on a thin layer chromatography (TLC) plate (*n*-hexane: DCM = 3:1). Pure $Au_{44}(TBBT)_{28}$ was scraped off the TLC plates and crystallized in toluene/methanol at room temperature for 3 days.

## 3. Synthesis of $Au_{40}(TBBT)_{24}$dppbe

10.0 mg of $Au_{44}$ was dissolved in 5 mL of toluene in a 25 mL round bottom flask. The solution was then placed in an oil bath with a temperature of 60 °C, followed by the addition of 0.4 mg of dppbe (~1.2 equivalent, dissolved in 1 mL of toluene), and the reaction was slowly stirred for 1 hour. After that, the solution was concentrated with a rotary evaporator and precipitated with the addition of methanol. The precipitate was further washed twice with methanol. The raw product was separated using a thin-layer chromatography plate. It was found that $Au_{44}$ had completely converted, and $Au_{40}$ showed as a green band. Crystallization of $Au_{40}$ was carried out by diffusing ethanol into the toluene solution of $Au_{40}$ at room temperature, and high-quality single crystals of $Au_{40}$ structure was obtained after about 7 days.

## 4. Measurement

The UV-vis absorption spectrum of the nanocluster solution in this work was obtained using a METASH UV-9000 spectrophotometer. The ESI-MS measurement was recorded using a Waters Xevo G2-XS Q Tof mass spectrometer. The morphologies of the catalysts were obtained using a JEM 2100 transmission electron microscope. The binding energy of the elements was obtained using a Thermo

ESCALAB 250 equipped with a monochromated Al Kα (1486.8 eV) 150 W X-ray source. Thermogravimetric analysis was carried out on a TG/DTA 6300 analyzer (Seiko Instruments, Inc.), under an atmosphere of anhydrous $N_2$ with a heating rate of 10 °C $\mathrm{min}^{-1}$.

## 5. Single-crystal X-ray diffraction

The single-crystal structure of the nanocluster was obtained using a Rigaku XtaLAB Synergy-R Diffraction equipped with a digital camera diffractometer comprising a microfocus rotating anode X-ray source (Cu Kα, $\lambda$= 1.54178 Å) and an HPC detector [HyPix-6000C] radiation for the crystal structures. Using Olex2, the structure was solved with the SHELXT structure solution program using Intrinsic Phasing and refined with the SHELXL refinement package using least squares minimisation. The solvent mask routine of the Olex2 software was implemented to remove the contributions of some disordered solvent molecules to the observed structure factors. The solvent mask was calculated and 589 electrons were found in a volume of 2785 $\text{Å}^3$ in 3 voids per unit cell. This is consistent with the presence of 3[$C_7H_8$], 3[$C_7H_8$], 0.5[$CH_3OH$] per asymmetric unit which account for 618 electrons per unit cell.

## 6. Preparation method of catalyst

$TiO_2$ was first dispersed in dichloromethane and then nanoclusters were added (with a weight fraction of 0.5 wt.% and 1.0 wt.% based on the weight of nanoclusters). The reaction mixture was stirred continuously for about 3 hours and the solvent was removed by centrifugation. The samples were dried in a vacuum oven and used as catalysts directly without further treatment.

## 7. Catalytic experiment

10 mg of photocatalyst was added into the aqueous solution of rhodamine B (15 mL, $2\times10^{-4}$ mol $L^{-1}$), and the reaction was proceeded under visible light irradiation (300 W xenon lamp with filter, l > 420 nm). The UV-vis absorption spectra of the solution were measured every 30 min and the absorbance values at 554 nm were recorded until rhodamine B is completely degraded.

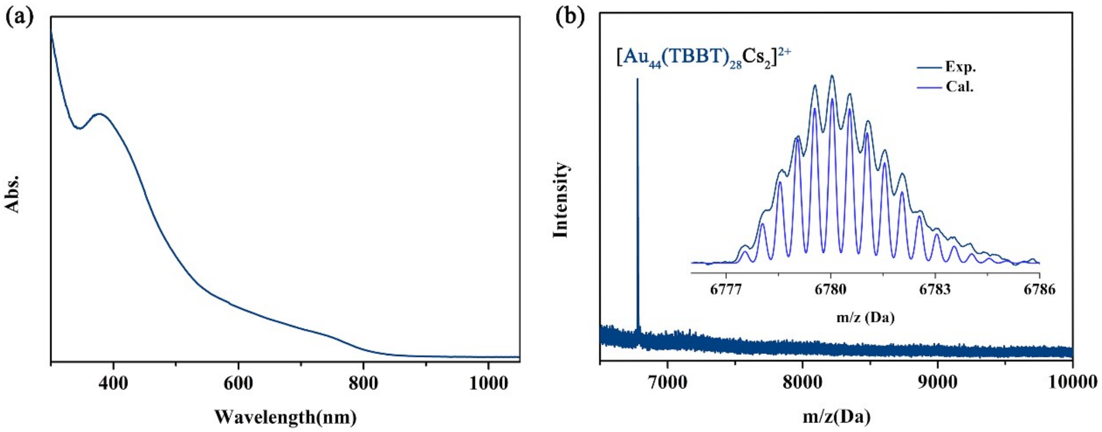

**Fig. S1** (a) UV-vis spectrum of $Au_{44}$; (b) ESI-MS of $Au_{44}$. Inset: isotopic pattern of the signal peak.

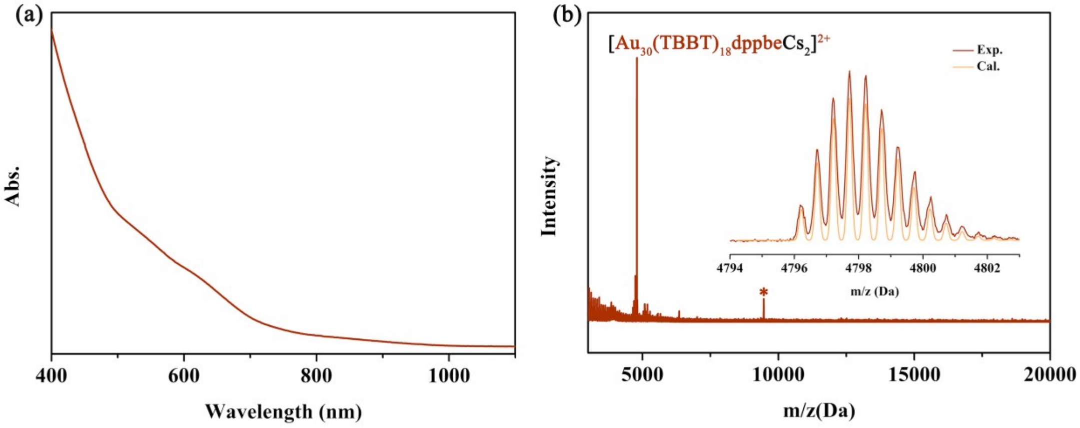

**Fig. S2** (a) UV-vis spectrum of $Au_{30}$; (b) ESI-MS of $Au_{30}$. Inset: Isotopic pattern of the signal peak. * indicates the signal peak of $[Au_{30}(TBBT)_{18}dppbe + Cs]^+$.

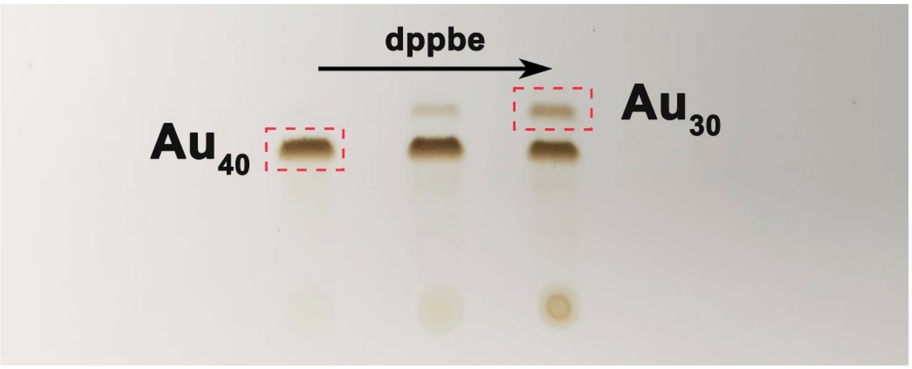

**Fig. S3** Photograph of the TLC plate showing the transformation from $Au_{40}$ to $Au_{30}$ with the addition of dppbe.

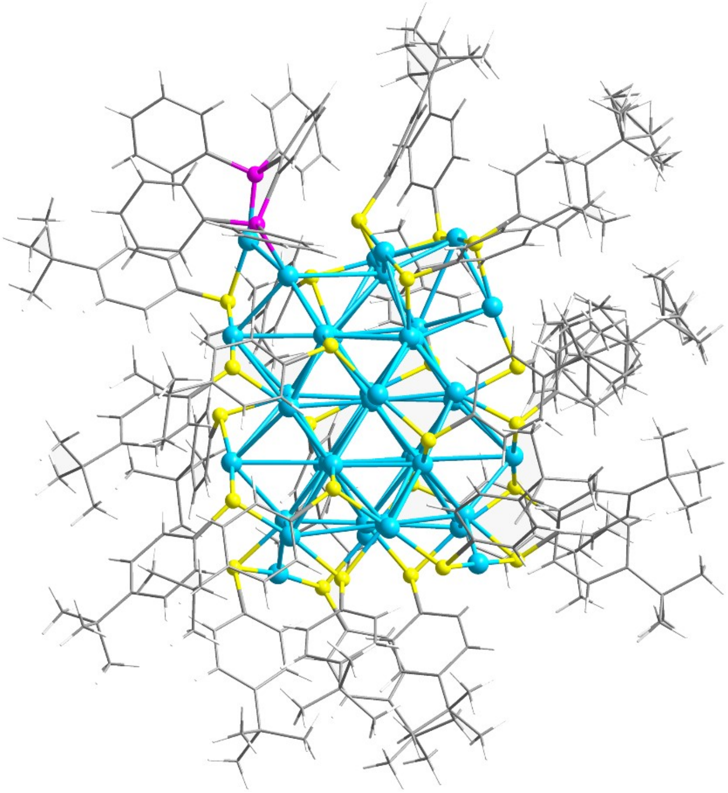

**Fig. S4** Total crystal structure of $Au_{40}$ nanocluster. (Label: Blue = Au; yellow = S; magenta = P; gray = C; white = H)

**Table S1.** Crystal data and structure refinement for $Au_{40}$

| | |
|---|---|
| CCDC code | 2412987 |
| Empirical formula | $C_{344}H_{422}Au_{40}O_{0.5}P_2S_{24}$ |
| Formula weight | 13274.83 |
| Temperature/K | 120.0 |
| Crystal system | triclinic |
| Space group | P-1 |
| a/Å | 19.7765(2) |
| b/Å | 22.8122(2) |
| c/Å | 41.4682(2) |
| α/° | 77.5200(10) |
| β/° | 89.8600(10) |
| γ/° | 76.3700(10) |
| Volume/Å$^3$ | 17728.5(3) |
| Z | 2 |
| $\rho_{calc}$g/cm$^3$ | 2.487 |
| μ/mm$^{-1}$ | 31.975 |
| F(000) | 12128.0 |
| Crystal size/mm$^3$ | 0.134× 0.118 × 0.088 |
| Radiation | Cu Kα (λ = 1.54184) |
| 2Θ range for data collection/° | 4.37 to 157.882 |
| Index ranges | $-25 \leq h \leq 24$, $-28 \leq k \leq 28$, $-52 \leq l \leq 52$ |
| Reflections collected | 238069 |
| Independent reflections | 72807 [$R_{int}$ = 0.1131, $R_{sigma}$ = 0.0752] |
| Data/restraints/parameters | 72807/2445/3500 |
| Goodness-of-fit on F$^2$ | 1.031 |
| Final R indexes [I>=2σ (I)] | $R_1$ = 0.0870, $wR_2$ = 0.2372 |
| Final R indexes [all data] | $R_1$ = 0.0967, $wR_2$ = 0.2450 |
| Largest diff. peak/hole / e Å$^{-3}$ | 4.38/-4.96 |

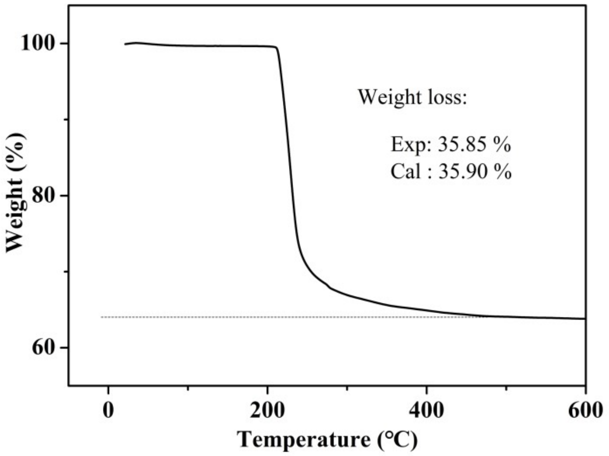

**Fig. S5** TGA result of $Au_{40}$ sample.

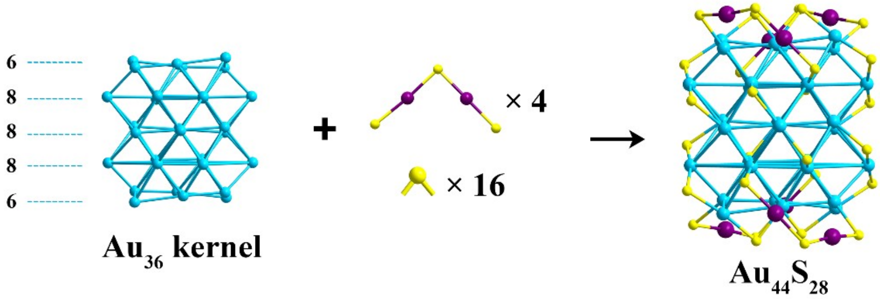

**Fig. S6** Structural analysis of the $Au_{44}$ nanocluster. (Label: Blue = Au in a kernel; violet = Au in a motif; yellow = S)

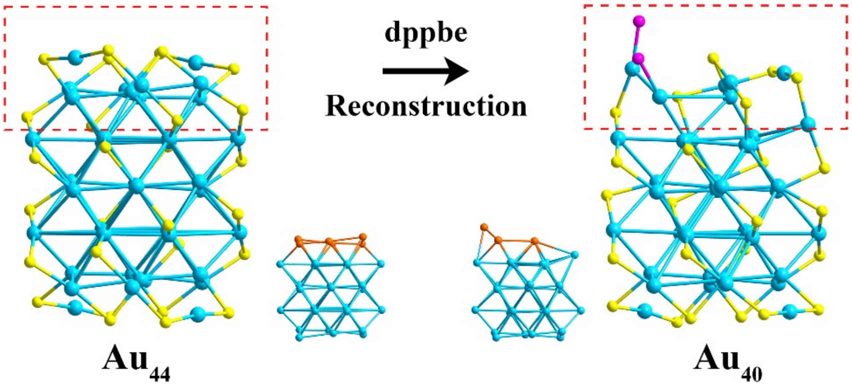

**Fig. S7** Structural comparison between $Au_{44}$ and $Au_{40}$, showing $Au_{40}$ as the derivative of $Au_{44}$ with the introduction of dppbe. (Label: Blue, orange = Au; yellow = S; magenta = P).

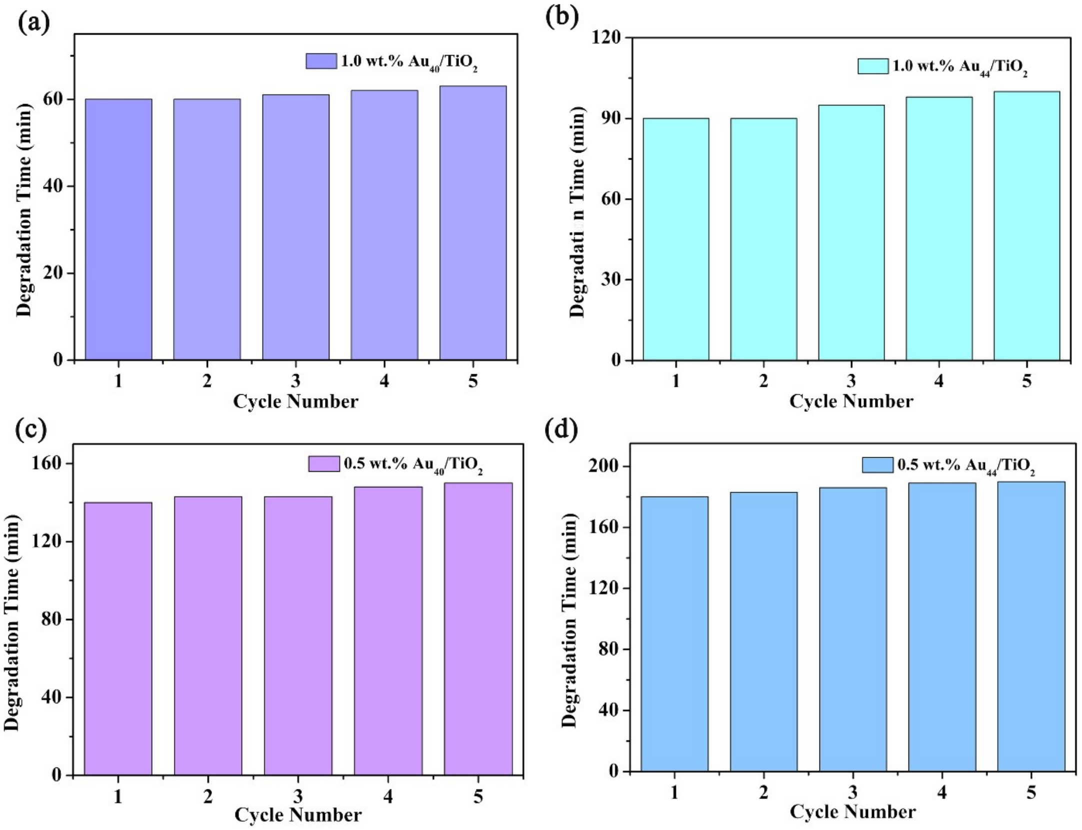

**Fig. S8** Complete degradation time of recycling catalytic experiments catalyzed with (a) 1.0 wt.% $Au_{40}/TiO_2$, (b) 1.0 wt.% $Au_{44}/TiO_2$, (c) 0.5 wt.% $Au_{40}/TiO_2$, (d) 0.5 wt.% $Au_{44}/TiO_2$.

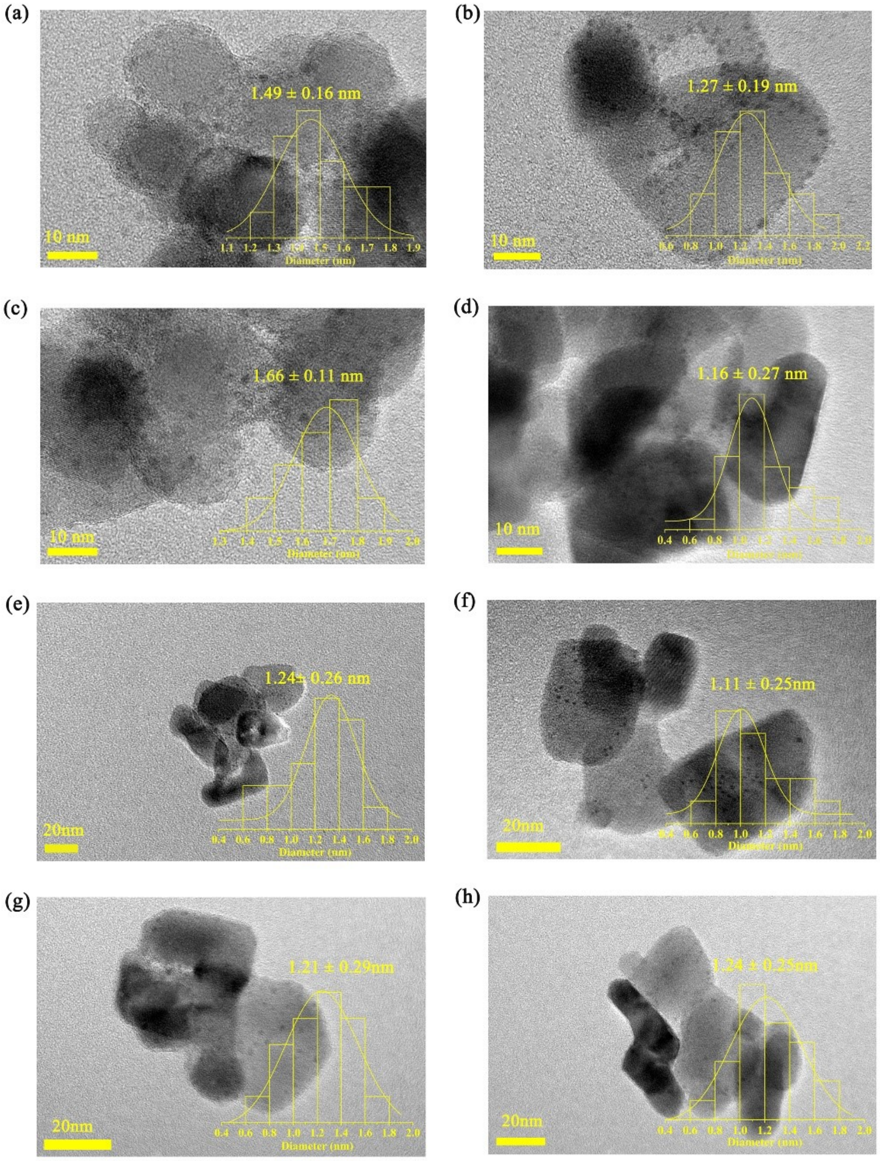

**Fig. S9** TEM images of the photocatalysts before the catalytic reaction: (a) 1.0 wt.% $Au_{40}/TiO_2$, (b) 1.0 wt.% $Au_{44}/TiO_2$, (c) 0.5 wt.% $Au_{40}/TiO_2$ (d) 0.5 wt.% $Au_{44}/TiO_2$; TEM images of the photocatalysts after the catalytic reaction: (e) 1.0 wt.% $Au_{40}/TiO_2$, (f) 1.0 wt.% $Au_{44}/TiO_2$, (g) 0.5 wt.% $Au_{40}/TiO_2$ (h) 0.5 wt.% $Au_{44}/TiO_2$. Insets: Size distribution of the NCs on the $TiO_2$.

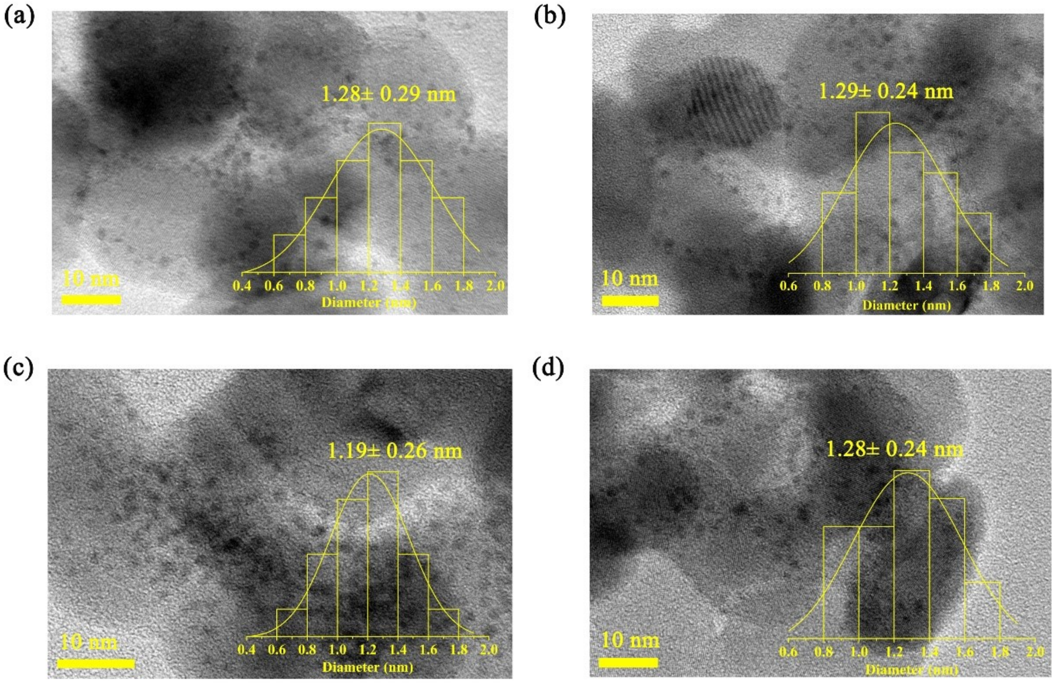

**Fig. S10** TEM images of the photocatalysts after five times catalytic reaction: (a) 1.0 wt.% $Au_{40}/TiO_2$, (b) 1.0 wt.% $Au_{44}/TiO_2$, (c) 0.5 wt.% $Au_{40}/TiO_2$ (d) 0.5 wt.% $Au_{44}/TiO_2$.

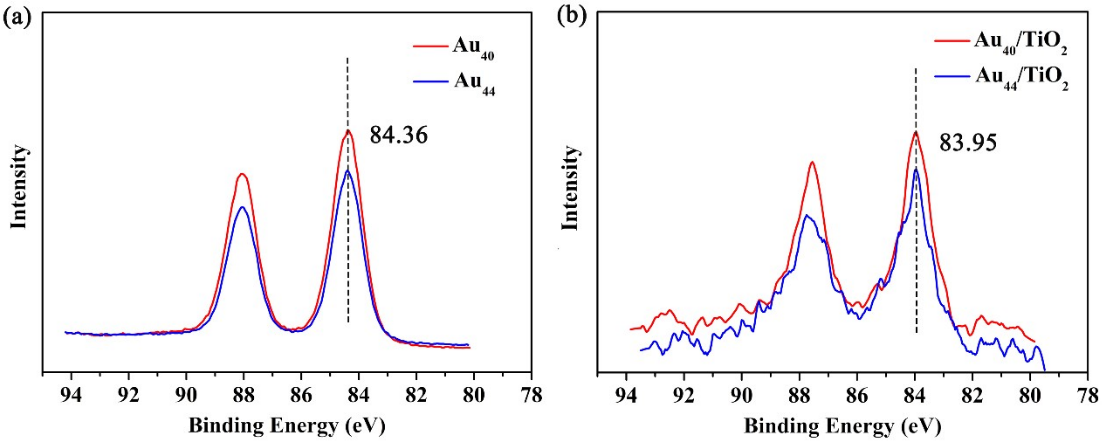

**Fig. S11.** XPS curves of the Au 4f bands of (a) support-free $Au_{40}$, $Au_{44}$ and (b) supported $Au_{40}$, $Au_{44}$.

## Reference

1. C. Zeng, Y. Chen, K. Iida, K. Nobusada, K. Kirschbaum, K. J. Lambright and R. Jin, *J. Am. Chem. Soc.*, 2016, **138**, 3950–3953.